Cancer Chemother Pharmacol (1996) 37: 305–316

ORIGINAL ARTICLE

**William T. Bellamy · Pamela Mendibles · Petra Bontje
Floyd Thompson Lynne Richter · Ronald S. Weinstein
Thomas M. Grogan**

Development of an orthotopic SCID mouse-human tumor xenograft model displaying the multidrug-resistant phenotype

Received: 3 December 1994 / Accepted: 9 May 1995

Abstract Multiple myeloma is a plasma cell malignancy which is generally incurable in spite of a high initial response to chemotherapy. While animal models of myeloma are known, the recent developments of human xenografts in nude and SCID mice suggests a promising experimental model. The SCID model, in particular, holds promise because these animals readily accept hematopoietic and lymphoid transplantation and do not generally develop graft versus host reaction. We have developed two drug-resistant variants of the human multiple myeloma cell line ARH-77 by in vitro exposure to gradually increasing concentrations of doxorubicin (ARH-D60) or mitoxantrone (ARM-80). When injected into irradiated SCID mice, the ARH-D60 cell line grew in an orthotopic pattern with the development of osteolytic lesions. This is in contrast to the 8226/C1N human myeloma cell line which grows in a disseminated but nonorthotopic manner in the SCID mouse. Both the ARH-D60 and ARM-80 cell lines are resistant to doxorubicin and cross-resistant to mitoxantrone, vinca alkaloids, taxol and m-AMSA while maintaining sensitivity to antimetabolites and alkylating agents. Growth characteristics and cell cycle kinetics, including S-phase, were not altered in the resistant sublines. The ARH-D60 and ARM-80 cell lines both displayed a classic multidrug-resistance (MDR) phenotype which was partially reversed by the addition of verapamil. These two cell lines represent the first MDR human myeloma cell lines which have demonstrated an orthotopic growth pattern in the SCID mouse and thus may be of value in studying the pathophysiology of this disease.

Key words Multidrug resistance · Multiple myeloma · SCID mouse

Abbreviations *PBS* phosphate-buffered saline (5 m*M* KH_2PO_4, 150 m*M* NaCl, pH 7.4) · *MTT* 3-(4,5-dimethyl thiazol)-2,5 diphenyltetrazolium bromide · *MDR* multidrug resistance · *SDS* sodium dodecyl sulfate · IC_{50} concentration resulting in 50% (80%) inhibition of cell growth · *5-FU* 5-fluorouracil · *EBNA* Epstein-Barr nuclear antigen · *DMSO* dimethyl sulfoxide · *MRP* multidrug resistance related protein · *SSC* 0.15 *M* sodium chloride/0.015 *M* sodium citrate · *G3PDH* glyceraldehyde-3-phosphate dehydrogenase · *SCID* severe combined immune deficiency · *ELISA* enzyme-linked immunosorbent assay · *ISCN* International System for Human Cytogenetic Nomenclature · *HSR* homogeneously staining region · *RT-PCR* reverse transcriptase-polymerase chain reaction · *FBS* fetal bovine serum · *DEPC* diethylpyrocarbomate · *BSA* bovine serum albumin

This work was supported in part by National Cancer Institute grants CA57228 and CA 23074 and ES06694.

W. T. Bellamy (✉) · P. Mendibles · L. Richter · R. S. Weinstein
T. M. Gorgan
Department of Pathology, College of Medicine, University of Arizona, 1501 N. Campbell Avenue, Tucson, AZ 85724, USA

P. Bontje
Free University, Amsterdam, The Netherlands

F. Thompson
Arizona Cancer Center, University of Arizona, College of Medicine, Tucson, Arizona, USA

Introduction

Multiple myeloma is a plasma cell malignancy which frequently involves bone, and is generally incurable in spite of a high initial response to chemotherapy [4]. Melphalan with or without prednisolone has been the standard myeloma treatment for more than 30 years [10] and produces objective responses in 40 to 60% of patients with a median survival of between 20 to 30 months [12]. The prognosis of patients with primary

resistance to chemotherapy and those who have relapsed after initial chemotherapy is generally poor. The VAD regimen (vincristine–doxorubicin–dexamethasone), introduced in the 1980s [3], is now widely used as second–line therapy. It generally produces a rapid tumor mass reduction [12] and has been found to be comparable to melphalan–prednisolone [1].

Two of the components of VAD, doxorubicin and vincristine, have been associated with the overexpression of P-glycoprotein and the development of multidrug resistance (MDR). The P-glycoprotein is a cellular efflux pump encoded by the *MDR*1 gene, and is responsible for the MDR phenotype [5]. Studies have indicated that end-stage myeloma patients commonly express P-glycoprotein [19]. Among those patients receiving VAD, the proportion of MDR1-positive cells has been shown to be higher in resistant than in responding patients [22]. It has been reported that P-glycoprotein is expressed in less than 5% of untreated myeloma patients and increases to approximately 70% in refractory patients [20]. A high cumulative dose of vincristine (> 20 mg) and doxorubicin (> 340 mg) appears to be highly predictive for P-glycoprotein expression [28].

Development and testing of novel therapies directed against human myeloma has been hampered by the lack of a suitable in vivo model. We have developed an in vivo model of MDR myeloma in SCID mice [7]. Myeloma serves as an excellent model for the study of in vivo drug resistance and chemomodulation for several reasons: (a) tumor cells are readily detected by virtue of their reliable immunoglobulin secretion; (b) the amount of immunoglobulin secreted into the urine is directly related to the amount of tumor burden, thereby allowing for ready calculation of therapy effects; and (c) human–SCID xenografts are readily attained. While animal models of myeloma are known, the recently developed of human xenografts in nude and SCID mice are a promising experimental model. The SCID model, in particular, holds promise because these animals readily accept hematopoietic and lymphoid transplantation and do not generally develop graft versus host reaction. The use of a clinically relevant animal model is necessary because many new cancer treatments may appear promising in vitro but are inactive or prohibitively toxic in patients. The SCID model is ideal for these proposed studies because it will allows consistent growth and spread of human tumors over a short period of time.

In this study, we describe the characteristics of doxorubicin- and mitoxantrone-resistant human myeloma cell lines derived from the well-established human myeloma cell line ARH-77 [11]. These cell lines were created to complement our 8226 human myeloma SCID mouse xenograft model [7]. One of these cell lines, the ARH-D60, grows in the SCID mouse in an orthotopic pattern. This ARH-D60 human myeloma–SCID xenograft model has substantial bone marrow-based disease which closely mimics the pathophysiology of human myeloma. This is in contrast to the 8226/C1N human myeloma cell line which grows nonorthotopically in the SCID mouse. These cell lines may be of value in studying the pathophysiology of MDR myeloma.

Materials and methods

Cell and culture conditions

The ARH-77 human myeloma cell line, obtained from the American Type Culture Collection (Rockville, Md.), was originally derived from the peripheral blood of a 33-year-old female with IgG, kappa plasma cell leukemia [11]. The ARH-77 cell line produces IgG_k and is EBNA positive [21] . Cells were grown in suspension in RPMI-1640 medium supplemented with 5% fetal bovine serum, 1% (v/v) penicillin (100 units/ml), streptomycin (100 μg/ml) and 1% (v/v) L-glutamine (Grand Island Biological Supply Co, Grand Island, N.Y.), and were maintained at 37° C in an atmosphere of 5% CO_2/95% air.

Drugs

Mitoxantrone was obtained from Lederle laboratories, Pearl River, N.Y. Taxol and m-AMSA were obtained from the Drug Synthesis and Chemistry Branch, Developmental Therapeutics Section, Division of Cancer Treatment, National Cancer Institute. All other drugs were purchased from Sigma Chemical Co., St. Louis, Mo. Drugs were prepared by dissolving in sterile water, DMSO, or, in the case of melphalan, acidified ethanol. The final concentration of ethanol was 0.01% when exposed to cells and was included in controls. [^{14}C]Mitoxantrone (specific activity 66 mCi/mmol) was a gift from Dr. Lee Greenberger, Lederle Laboratories. [^{3}H]Vinblastine (specific activity 8.3 Ci/mmol) was obtained from Amersham (Arlington Heights, IL) and [^{3}H]daunorubicin (specific activity 2.0 Ci/mmol) from New England Nuclear (Cambridge, Mass.).

Selection of drug-resistant cells.

ARH-77 (ARH-77/S) cells were initially exposed to either doxorubicin or mitoxantrone at a concentration of 1×10^{-8} M, which represented the approximate IC_{80} concentration. Fresh drug was added to the medium whenever it was changed (approximately three times weekly). Drug exposure was gradually increased to a final concentration of 6×10^{-7} M (ARH/D60) or 8×10^{-7} M (ARM-80). Cells were maintained in a drug-free medium for 1 week prior to any experiments.

Cell growth characteristics

For the determination of doubling time, growth curves were established for each cell line by plotting cell number versus growth time. Doubling time was determined directly from the linear portion of the plot. To assess possible differences in cell size, cells were fixed in Krishan's buffer (0.1% sodium citrate, 5.0 mg RNase A, 0.3% NP-40 detergent, and 12.5 mg propidium iodide in 250 ml distilled H_2O), pH 7.4. Cells were analyzed on a water-cooled Becton Dickinson FACS $Star_{PLUS}$ instrument (Mountain View, Calif). Data were collected in linear mode, and analyzed with CONSORT 40 software using the cotfit program, on a DEC microVMS computer

(Merrimac, N.H.). The fraction of cells in S-phase of the cell cycle was determined using flow cytometry after propidium iodide staining of the cells [32].

Immunocytochemistry

Cytospins were prepared from the ARH cell lines and the cells evaluated for expression of the plasma cell antigens PCA-1 (Coulter Immunology, Hialeah, Fl.) and CD-38 (Leu 17) (Becton Dickinson, Mountain View, Calif.). Expression of P-glycoprotein was evaluated with monoclonal antibodies C-494 and JSB-1 (Signet Laboratories, Dedham, Mass.) using a previously described immunocytochemical method [27]. By this same method, the monoclonal antibody Ki-67 (DaKopatts, Copenhagen) was used to detect a nuclear proliferation antigen as a measure of proliferative activity of tumor cells [26]. Other antigens investigated included kappa and lambda light-chain expression, CD-56 (NCAM) and CD-45 (HLe-1). An irrelevant isotype-matched, concentration-matched primary antibody was substituted as a negative control.

In vitro cytotoxicity assays

A colorimetric assay based on the ability of viable cells to reduce the tetrazolium salt, MTT (3-[4,5-dimethylthlazol-2-yl]-2,5-diphenyl tetrazolium), to a blue formazan product was used to measure cytotoxicity following exposure to drug [13]. Cells were plated into 96-well microtiter plates (Falcon, Becton Dickinson, Oxnard, Calif.) at 10,000 cells/well in 0.2 ml of medium containing appropriate concentrations of drug with six replicates. In certain experiments, verapamil (10 μ*M*) was added 15 min prior to the addition of cytotoxic drug and was present continuously during the period of incubation. After incubation for 4 days at 37° C, 50 μl of MTT dye (2 mg/ml) was added to each well and incubated for 4 h. Plates were then centrifuged at 500 *g* for 5 min medium aspirated and dimethyl sulfoxide added to each well (100 μl). The plates were mechanically agitated for 5 min and the optical density at 540 nm determined on a microplate reader (Bio-Tek EL-311, Bio-Tek Instruments, Laguna Hills, Calif.). Data were expressed as the percentage of the optical density value obtained for untreated cells at 540 nm corrected for background absorbance. The surviving fraction of cells was determined by dividing the mean absorbance values of the drug-treated samples by the mean absorbance values of untreated control samples. The IC_{50} for each drug, defined as the concentration of drug which reduces growth to 50% of untreated control cells, was calculated from linear transformation of the dose response curves. A relative resistance index was expressed as the ratio of the IC_{50} of the resistant cells to the IC_{50} of the sensitive parental cell line. Each experiment was repeated a minimum of three times.

Cytogenetic studies

Cell lines were harvested by standard methods as previously described [38, 40], and karyotype abnormalities of the modal (i.e. predominant) populations were described according to ISCN recommendations [30]. On average, a total of 30 metaphase cells per harvest were counted while six G-banded karyograms were prepared for description of clonal chromosomal abnormalities.

Drug accumulation studies

To determine drug accumulation, cells were studied in the exponential growth phase. The cells were washed free of medium and resuspended at a concentration of 1×10^6 cells/ml in RPMI-1640 medium containing 5% FBS. Radiolabelled drug was added to each tube of cells and the cells incubated in a water bath at 37° C for 60 min. Following incubation, the cells were placed on ice and diluted with iced PBS, pH 7.4, pelleted and washed again with PBS. After the final wash, the cells were resuspended in 0.5 ml PBS and transferred to scintillation vials where they were digested with 0.2 N NaOH followed by neutralization with 1 N HCl. Scintillation fluid was added and the amount of radiolabel (cpm) was determined using liquid scintillation counting (Beckman LS6000, Beckman Instruments, Fullerton, Calif.). Results are expressed as cpm/1×10^6 cells. Each experiment was repeated a minimum of three times. For all experiments involving verapamil, cells were incubated in medium containing 10 μ*M* verapamil for 15 min prior to and throughout the period of drug exposure.

Southern blot analysis

Genomic DNA was extracted from the ARH cell lines using a DNA isolation kit (Oncor, Gaithersburg, Md.) according to the manufacturer's instructions. DNA (10 μg) from each cell line was digested with EcoRI or HindIII with placental DNA included as a control. The digests were run on a Probe Tech 1 electrophoresis/vacuum transfer apparatus (Oncor) overnight at 19 V. Following ethidium bromide staining and photography, the gel was placed back in the Probe Tech, depurinated for 15 min, denatured for 30 min, and the DNA was transferred to a charged nylon membrane (Oncor) by applying a vacuum for 90 min. The DNA was crosslinked to the membrane by UV irradiation (Stratalinker, Stratagene, LaJolla, Calif.). The blot was prehybridized in Hybrisol I (Oncor) at 45° C for 1 h followed by overnight hybridization at 45° C with the human MDR1 cDNA probe, pHDR5α [41], which had been random primed with ^{32}P α-dCTP according to the method of Feinberg and Vogelstein [24]. Stringency washes were carried out in 0.1 × SSC, 0.1% SDS with two washes at room temperature for 15 min each and a final wash at 52° C for 90 min.

Northern blot analysis

RNA was isolated from the ARH cell lines using guanidium isothiocynate and cesium chloride gradient centrifugation according to the method of Chirgwin et al. [14]. Absorbance at 260 nm was used to quantitate the RNA. Total cellular RNA (5 μg/lane) was denatured at 65° C for 10 min in 50% formamide, 6.5% formaldehyde and 40 m*M* 3-(*N*-morpholino)propanesulfonic acid, and subjected to electrophoresis on a 1% formaldehyde agarose gel. The RNA was transferred to a nylon membrane (Nytran, Schleicter & Scheull, Keene, N.H.) in 20 × SSC overnight and immobilized by exposure to UV radiation as described above. Filters were prehybridized in Rapid-hyb buffer (Amersham, Arlington Heights, Ill.) according to the manufacturer's instructions. Hybridization was carried out at 42° C for 24 h with ^{32}P-labelled cDNA probes complementary to human MDR1 (pHDR5α) or MRP [15]. Following stringency washes, the filters were exposed to X-ray film (Kodak, X-OMAT) at − 80° C with an intensifying screen. To normalize for loading differences, the filters were hybridized with a human G3PDH cDNA probe (Clontech, Palo Alto, Calif.).

In situ hybridization

Paraffin sections were cut 4 μm thick and heated at 60° C for 2 h. The sections were then deparaffinized in two changes of xylene for 12 min each, two changes of 100% ethanol for 5 min each, and were taken through a graded series of alcohols (95%, 80%, 70%) followed by two changes of DEPC H_2O. Proteinase K (100 μg/ml, Boehringer-Mannheim, Indianapolis, Ind.) was then placed on the sections for 60 min at 37° C and removed by two washes in PBS followed by

dehydration through a second series of graded alcohols (70%, 80%, 95%, 100%). The slides were allowed to air dry prior to hybridization. The slides were heated to 95° C and hybridization to a biotinylated human DNA probe enriched for the repetitive *Alu* and *Kpn* sequences (Cot-1, Gibco BRL, Grand Island, N.Y.) was carried out in 25% formamide, 10% dextran sulfate, 5 × Denhardt's, 4 × SSC, 50 m*M* sodium phosphate (pH 7.0), 1 m*M* EDTA, and 100 µg/ml salmon sperm DNA overnight at 37° C. Two stringency washes of 2.5% BSA, 0.1 × SSC were carried out at room temperature for 10 min each. The slides were then washed in PBS and blocked with 1% BSA in PBS for 30 min at room temperature. For detection of the biotinylated probe, the ExtrAvidin Alkaline Phosphatase system was used according to the manufacturer's protocol (Sigma Immunochemicals, St. Louis, Mo.).

Generation of human multiple myeloma in SCID mice

BALBc/C.17 mice homozygous for the SCID defect (scid/scid) were bred and maintained in a dedicated facility at the Arizona Health Science Center. Principles of animal care as set forth in NIH publication no. 85-23, rev. 1985, were followed throughout. The animals were housed in microisolator cages under specific pathogen-free conditions and were handled in a laminar flow hood. They were fed LM45 5% fat, autoclavable pellets (Tekland Premier, Madison, Wis.) and given autoclaved water supplemented with antibiotics. Mice were screened at regular intervals for the presence of bacteria, Sendai virus, mouse hepatitis virus and mycoplasma. All mice were evaluated for the presence of mouse IgG by ELISA assay and only those animals with ≤ 1 mg/l of mouse Ig were used. Male and female animals at 5–8 weeks of age were used for all studies. Prior to injection, the cells were washed twice and resuspended in sterile PBS, pH 7.4. In all instances, low passage number cells in logarithmic growth were used. Each animal received a total of 25×10^6 ARH-D60 or ARH-77 cells as a single intravenous injection in the tail vein. The animals were exposed, 24 h prior to injection of the cells, to a sublethal dose of radiation (200 cGy) from a ^{60}Co source. Autopsies were performed on the mice approximately 30 to 40 days after cell inoculation to obtain tissues for histological examination and immunophenotyping as previously described [7].

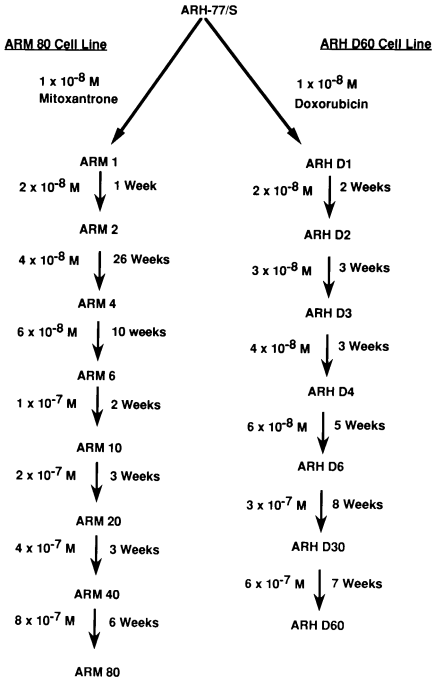

Fig. 1 Multistep selection procedure for isolating the ARH-D60 and ARM-80 sublines from ARH-77 human myeloma cells. Cells were selected and maintained at a fixed concentration until they demonstrated an adaptive growth pattern. The time period at a given concentration is given to the right of the arrow.

Table 1 Cell growth characteristics. Values are means ± SD

	ARH-77/S	ARH-D60	ARM-80
Cell size[a]	1.0	0.97	0.96
Doubling time (h)	45.5 ± 10	30.6 ± 5.4	35.8 ± 11.4
% S-Phase	30.8 ± 0.6	30.6 ± 5.4	35.8 ± 11.4

[a] Normalized to 1.0 for the ARH-77/S cell line, determined using flow cytometry

Results

Selection of drug-resistant cell lines

We have developed two drug-resistant variants of the human multiple myeloma cell line ARH-77 through in vitro exposure to doxorubicin (ARH-D60) or mitoxantrone (ARM-80). The parental ARH-77 cells (ARH-77/S) were initially exposed to either drug at a concentration of 1×10^{-8} M, which represented the approximate IC_{80} and the concentration of each drug was slowly increased in a multiple step procedure as shown in Fig. 1. Fresh drug was added whenever the medium was changed (approximately three times weekly). Over a period of 28 weeks the concentration of doxorubicin was increased from 1×10^{-8} M to 6×10^{-7} M, representing a 60-fold increase in the selection pressure, with the cell line derived from this concentration designated as ARH-D60. The mitoxantrone-resistant cell line, ARM-80, was selected in a similar fashion by increasing the drug concentration from 1×10^{-8} *M* to 8×10^{-7} *M* over a 51-week period, an 80-fold increase in the initial selection pressure.

Despite the development of drug resistance, both of the ARH sublines retained several biological characteristics of the parental ARH-77 cell line. The growth characteristics of the parental cell line, ARH-77/S , and the two drug-resistant sublines, ARH-D60 and ARM-80, are listed in Table 1. The population doubling times were similar and there was no significant difference between the three cell lines when the percentages of cells in S-phase of the cell cycle were compared. For the determination of doubling time, cell growth curves were established for each cell line by plotting cell number versus growth time and the doubling time determined directly from the linear portion of the plot. The doubling time of the ARH-77 parental cell line was determined to be 45 ± 10 h while that of the ARH-D60 subline was 30 ± 5 h and the ARM-80 subline was 35 + 11 h.

Table 2 Immunophenotype of ARH cell lines

	ARH-77/S	ARH-D60	ARM-80
κ Light chain	Pos.	Pos.	Pos.
λ Light chain	Neg.	Neg.	Neg.
IgG	Pos.	Pos.	Pos.
CD-38 (Leu17)	Pos.	Pos.	Pos.
CD-45	Pos.	Pos.	Pos.
CD-56 (N-CAM)	Neg.	Neg.	Neg.
JSB-1	Neg.	Pos.	Pos.
C-494	Neg.	Pos.	Pos.

Immunophenotyping of ARH cell lines

Cytospins were prepared from the ARH cell lines and the cells evaluated for expression of a variety of plasma cell and drug-resistance markers. Both drug-resistant sublines had a plasma cell morphology and expressed the plasma cell-associated antigens PCA-1 and CD38. There was no alteration in the expression of the nuclear proliferative antigen, Ki-67, with greater than 90% of the cells in both the drug-sensitive and -resistant sublines expressing this antigen. As expected, all three cell lines stained positive for kappa and negative for lambda light-chain expression. Both the ARH-D60 and ARM-80 sublines were positive for CD-45 expression and were negative for CD-56, findings which were identical to the parental cell line. The two drug-resistant cell lines differed from the parental phenotype by staining positive for P-glycoprotein expression using monoclonal antibodies C-494 and JSB-1. The results of the immunophenotyping are presented in Table 2.

Cytogenetics

Karyotype abnormalities are summarized in Table 3. Cell lines were harvested by standard methods and karyotype abnormalities of the modal (i.e. predominant) populations were described according to ISCN recommendations. On average, a total of 30 metaphase cells per harvest were counted while six G-banded karyograms were prepared for description of clonal chromosomal abnormalities. ARH-77 was a very homogeneous diploid cell line with a mode of 46 (64% of cells counted) and the range of counts was 43–46. However, the karyotype contained a number of translocations (e.g. between chromosomes 2 and 5, 2 and 3, 3 and 5, 3 and 9, 6 and 22, 9 and 17, and 15 and 11), and an isochromosome for the short arm of chromosome 9. The translocations resulted in deletions of chromosomal segments which included the centromere of chromosomes 5, 11, and 17, and loss of the centromere resulted in these chromosomes being technically listed as lost (i.e. -5, -11, -17) according to ISCN [30]. The ARH-D60 cell line was similarly near diploid with a mode of 46 (56% of cells examined) and a range of counts between 44 and 46. The ARH-D60 karyotype, relative to the parental line ARH-77, revealed a gain of normal chromosomes 5, 11, and 15, a loss of the translocation chromosome t(11;15), and a gain of a number of additional structural abnormalities while retaining the other rearrangements seen in ARH-77. The most interesting structural abnormality present was a derivative chromosome 7 which displayed a homogeneously staining region (HSR), a karyotypic anomaly known to often result from gene amplification (see Fig. 2). Additionally, there was a sideline which had a similar appearing HSR on one arm of an isochromosome (13q), and nonclonal abnormalities seen in single karyograms which involved apparent "jumping" translocations of the HSR to different chromosome partners. The revertant cell line, ARH-D60-Rev, while still having a mode of 46 (39% of cells), was more heterogeneous, having a range of counts between 40 and 47. The predominant (i.e. modal) karyotypes of this cell line were essentially identical to ARH-D60. However, there was a population of cells which lost the HSR-bearing chromosome.

The mitoxantrone-selected cell line, ARM-80, was very heterogeneous, but had several structural abnormalities which were similar to those observed in the ARH-D60 cell line including: t(2;3), t(3;5)(p13;p13), del(6), t(6;22), and i(13q). Unique structural

Table 3 Summary of cytogenetic findings in the ARH-77/S, ARH-D60 ARH-D60-Rev subline, and ARM-80 cell lines. Bold type indicates chromosomal abnormalities in the doxorubicin-resistant lines which are different from the parental ARH-77. Underlined type in the revertant karyotype interpretation highlights the finding of a sideline population within this specimen which has lost the HSR-bearing chromosome.

Cell Line	Karyotype
ARH-77/S	44, XX, der(2)t(2;5)(q24;q31), der(3)t(2;3)(q24;p26), der(3) t(3;5)(p13;p13), -5, del(6)(p22), der(9)t(3;9)(p23;p13),der(9) t(9;17)(p13;q21), + i(9)(p10), -11, der(15)t(11;15)(q11;p11),-17, der(22)t(6;22)(p22;q13)
ARH-D60	46, X, **add(X)(p11)**, der(2)t(2;5) (q24;q31), der(3)t(2;3)(q24;p26), der(3)t(3;5)(p13;p13), del(6) (p22), **der(7)dup(7)(q21q36) hsr(7)(q21)**, der(9)t(3;9) (p23;p13), der(9)t(9;17) (p13;q21), **dup(12)(q24)**, + i(9)(p10), **i(13)(q10)**, -17, der(22)t(6;22)(p22;q13) [5]/42-46, idem, -i(13)(q10), **der(13) i(13)(q10)hsr(13)(q34)** [cp2]
ARH-D60-Rev	46, X, **add(X)(p11)**, der(2)t(2;5) T93-(q24;q31), der(3)t(2;3)(q24;p26), der(3)t(3;5)(p13;p13), del(6)(p22), **der(7)dup(7)(q21q36) hsr(7)(q21)**, der(9)t(3;9) (p23;p13), der(9)t(9;17) (p13;q21), **dup(12)(q24)**, + i(9)(p10), i(13)(q10), -17, der(22)t(6;22)(p22;q13) [10]/43-46, idem, -der(7)dup(7)(q21q36)hsr(7)(q21) [cp7]
ARM-80	41-45, X, -X, der(2)t(2;5) (q24;q31), der(3)t(3;5)(p13;p13), dic(3;5)(p26;p13), i(4)(q10), del(6)(p22), hsr(7)(q31), add(7)(q31), der(9)t(9;17) (p13;q21), dup(12)(q24), i(13)(q10), add(14)(q32), der(22)t(6;22)(p22;q13) [cp5]

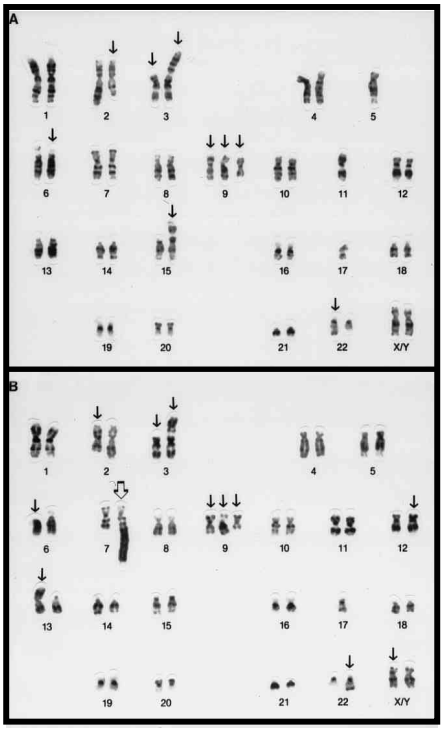

Fig. 2A, B Representative G-banded karyotypes of (**A**) ARH-77, and (**B**) ARH-D60. *Small solid arrows* indicate clonal structural abnormalities. *Larger open arrow* points to derivative chromosome 7 with an HSR on the long arm. The ARM-80 cell line also contained an HSR on the long arm of chromosome 7 (not shown)

abnormalities in the ARM-80 cell line included a new translocation between chromosome 3 and 5, isochromosome 4(q), unidentified translocations to the long arm of chromosome 7 and to the terminus of the long arm of chromosome 14, and two marker chromosomes of unknown origin. Additionally, there was an HSR on one of the chromosome 7 homologs which occurred at a different chromosomal band and which appeared to be much longer than that seen in the ARH-D60 cell line.

Cross-resistance profile

The sensitivities of the three ARH cell lines to a number of chemotherapeutic agents was determined by the MTT assay. The data are expressed as the relative resistance of the ARH-D60 and ARM-80 cell lines as compared to the parental ARH-77/S cell line. The relative resistance value represents the IC_{50} of the resistant cell line divided by the IC_{50} of the parental line. As shown in Table 4, the ARH-D60 cell line was approximately 76-fold resistant to doxorubicin and was cross-resistant to mitoxantrone (14-fold), vinblastine (843-fold), vincristine (920-fold), taxol (113-fold) and m-AMSA (7-fold). The ARH-D60 cells maintained their sensitivity to antimetabolites and alkylating

Table 4 Drug resistance profile of ARH myeloma cell lines. Level of resistance = IC_{50} of drug resistant cell line/IC_{50} of drug sensitive cell line. IC_{50} values determined by MTT assay (*ND* not done)

Drug	ARH-D60	ARM-80
Doxorubicin	76	10
Daunorubicin	131	6.2
Mitoxantrone	14	4.8
Vincristine	920	1240
Vinblastine	843	529
Taxol	113	169
m-AMSA	7.1	ND
Melphalan	0.9	1.1
Methotrexate	1.1	1.3
ara-C	0.7	1.3
5-FU	0.9	1.3

agents. Although the selection pressure was higher and for a longer period of time for the ARM-80 cell line than the ARH-D60 subline, the ARM-80 cells displayed a lower overall level of drug resistance. They were approximately five fold resistant to the selecting agent mitoxantrone and were cross-resistant to the same agents as the ARH-D60 cell line with the exception of an observed tenfold resistance to ara-C. Significant resistance to vinca alkaloids and taxol was observed for both the ARH-D60 and ARM-80 cells.

When the ARH-D60 cells were cultured in drug-free medium for 28 weeks, a revertant cell line was obtained. Cytotoxicity studies were carried out on these cells, designated ARH-D60-Rev, and compared with those of ARH-D60 cells which were routinely cultured in the presence of doxorubicin. The results of the MTT assay revealed that the level of resistance to doxorubicin dropped from 76 to 18-fold when the cells were maintained in drug-free medium for 28 weeks. When cells were tested following 15 weeks in drug-free medium, no changes in cytotoxicity to doxorubicin nor MDR1 expression were noted. We are currently developing a revertant cell line for the ARM-80 phenotype.

The addition of 10 μM verapamil only partially reversed drug resistance to doxorubicin, vincristine, and mitoxantrone in these two cell lines. Verapamil alone was minimally toxic to the cells in the concentration used in these studies producing less than 10% cytotoxicity (data not shown). With the addition of verapamil, the IC_{50} of vincristine against the ARH-D60 cell line decreased approximately 31-fold while that of the ARM-80 cell line decreased 14-fold. Figure 3 presents a dose-response curve of the ARH cell lines to vincristine in the presence and absence of verapamil. The ARH-D60 cell line was 920-fold resistant to vincristine. When 10 μM verapamil was added to the medium 15 min prior to the addition of drug, the level of resistance fell to 29-fold. Similar findings were observed for the ARM-80 cell line. In the absence of verapamil the cells were 1240-fold resistant to vincristine while in its presence they were 88-fold resistant. The ARH-77/S

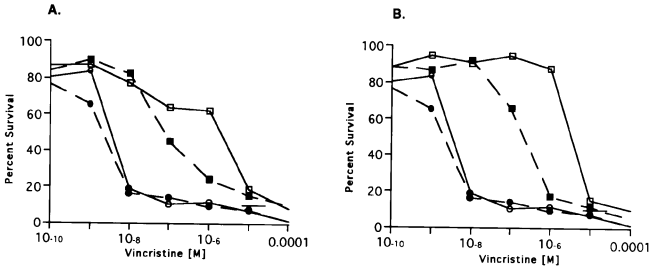

Fig. 3A, B Dose response curve of ARH cell lines to vincristine in the presence (*closed symbols*) or absence (*open symbols*) of 10 μ*M* verapamil. **A** ARH-D60 cell line; **B** ARM-80 cell line. Cytotoxicity was determined by the MTT assay.

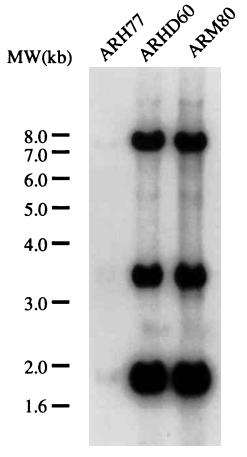

Fig. 4 Southern blot hybridization of Eco-RI-digested genomic DNA from ARH-77 and its MDR sublines. Each lane contained 10 μg of digested DNA and was hybridized with pHDR5α cDNA as described in the Materials and methods. Size markers were the BRL 1-kb DNA ladder (*kb* kilobase pairs)

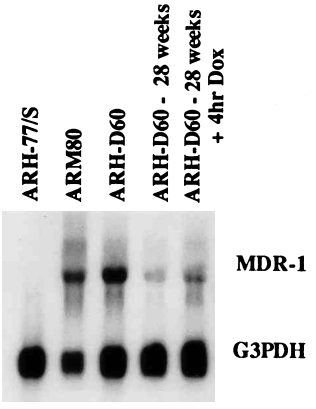

Fig. 5 Northern blot analysis of *MDR*-1 expression in the ARH-77 cell lines. Total cellular RNA (5 μg) was loaded in each lane and fractionated in a 1% agarose-formaldehyde gel. The northern blot was probed with a ^{32}P-labelled cDNA probe, pHDR5α. ARH-D60 cells were maintained in drug-free medium for 28 weeks (*lane 4*) and pulsed with $1 \times 10^{-6} M$ doxorubicin for 4 h prior to isolation of RNA (*lane 5*). Expression of G3PDH was used to assess RNA loading

cells were unaffected by the addition of verapamil. Both drug-resistant cell lines displayed identical patterns of reversal with doxorubicin and mitoxantrone. In each instance, verapamil was unable to completely reverse drug resistance. Escalation of the concentration of verapamil resulted in direct cytotoxicity to the cells. We are currently evaluating the ability of other modulators of the MDR1 gene for their ability to reverse drug resistance in these cells.

MDR1 expression

Genomic DNA was extracted from the ARH cell lines and digested with EcoRI or HindIII. Southern blot analysis was then carried out on the digests using the human MDR1 probe, pHDR5α. The results revealed that the MDR1 gene was amplified in both of the drug-resistant cell lines (Fig. 4)

Northern blot analysis also demonstrated that the MDR1 message was elevated in both of the drug-resistant cell lines, in concordance with their immunophenotype and cross-resistance profile (Fig. 5). As shown in Fig. 5, the MDR1 message was not detected in the parental cell line and additional studies using RT-PCR failed to detect it as well (data not shown). Expression of the MRP gene was also studied by northern blot analysis and was not found to be elevated in either of the two drug-resistant cell lines relative to the parental cells (data not shown). When the ARH-D60 cells were maintained in drug-free medium for 28 weeks, there was a noticeable decrease in the MDR1 message. When these cells, ARH-D60-Rev, were pulsed with doxorubicin for 4 h immediately prior to isolation of RNA, there was a slight increase in the expression of the MDR1 message. Studies are being carried out to determine if the P-glycoprotein is increased in these cells under these conditions.

Drug accumulation

To determine cellular accumulation of drug in the ARH-77 sublines, cells were studied in the exponential growth phase. The cells were washed free of medium and resuspended at a concentration of 1×10^6 cells/ml in RPMI-1640 medium containing 5% FBS. Radiolabelled drug ([^{14}C]mitoxantrone, [^{3}H]vinblastine, or [^{3}H]daunorubicin) was added to each tube of cells at 10 μ*M*, and the cells incubated in a water bath at 37° C for 60 min. The net intracellular accumulations of [^{3}H]daunorubicin, [^{3}H]vinblastine and [^{14}C]mitoxantrone following a 1-h drug exposure are displayed in Fig. 6. In both the ARH-D60 and ARM-80 cell lines, accumulation of daunorubicin, vinblastine and

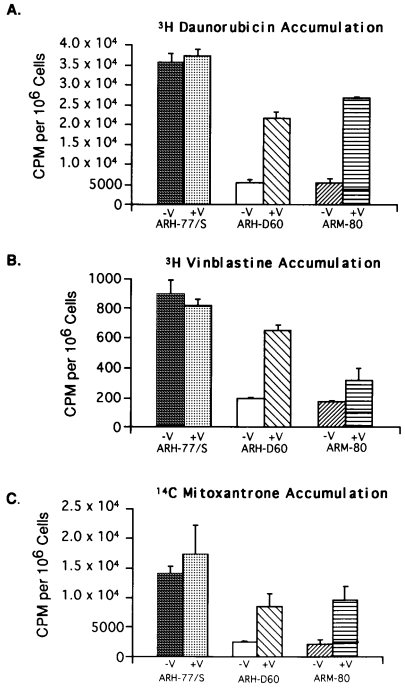

Fig. 6A–C Net drug accumulation after 1 h in ARH cell lines. Suspensions of cells (1×10^6 cells/ml) were exposed to 10 μ*M* (**A**) [^{3}H]daunorubicin, (**B**) [^{3}H]vinblastine or (**C**) [^{14}C]mitoxantrone for 1 h at 37° C with or without the addition of verapamil (10 μ*M*). Cells were then diluted in iced PBS, washed, lysed and accumulation determined by liquid scintillation counting. Results are expressed as cpm per 1×10^6 cells. The decreased accumulation of each of the three drugs alone in the ARH-D60 and ARM-80 cells relative to ARH-77/S cells was statistically significant ($P < 0.05$ in each case)

mitoxantrone was decreased relative to the ARH-77/S cell line. Nonspecific surface drug adsorption was assessed by measuring the binding at 0° C after exposure to 10 μM drug and immediately assaying for drug accumulation. A negligible amount of drug was found to be bound under these conditions. Accumulation was increased in the ARH-D60 and ARM-80 cell lines by the addition of 10 μ*M* verapamil, although not to the levels attained in the parental cell line. These results are in agreement with our cytotoxicity findings which showed that verapamil failed to completely reverse drug resistance in these cells.

Growth of ARH cells in SCID mice

When nonirradiated SCID mice were injected i.v. with ARH-77 and ARH-D60 cells there was no tumor growth (none of five mice). However, when SCID mice were irradiated with 200 rads from a ^{60}Co source followed by i.v. inoculation of cells 24 h later, 100% of the mice (28 of 28) developed tumors as assessed by detection of human kappa light-chain in the urine. Human kappa light-chain was detected in the urine within 7 days after inoculation and increased with time.Many of the mice developed hind leg paralysis (15 of 28) as a result of compression of the spinal cord by tumor. Histological analysis confirmed that myeloma cells proliferated and formed osteolytic lesions in the vertebrae (15 of 28) and skull (4 of 28). As presented in Table 5, tumor cells also invaded the liver (7 of 28), skeletal muscle (15 of 28), peritoneum (15 of 28) and kidney (6 of 28). There was no difference in either the

Table 5 Growth and distribution of ARH myeloma cells in SCID mice. values are the number of positive mice/total number of mice injected

	1×10^{7a}		5×10^{7a}	
	ARH-77	ARH-D60	ARH-77	ARH-D60
Liver	0/7[b]	1/7	2/7	4/7
Kidney	0/7	2/7	2/7	2/7
Spleen	0/7	0/7	0/7	0/7
Lung	0/7	0/7	0/7	0/7
Heart	0/7	0/7	0/7	0/7
Sk. Muscle	4/7	3/7	4/7	4/7
Peritoneum	6/7	1/7	4/7	4/7
Skull	0/7	0/7	2/7	2/7
Vertebrae	4/7	3/7	4/7	4/7
Hind Leg Paralysis	4/7	3/7	4/7	4/7

[a] Number of cells injected

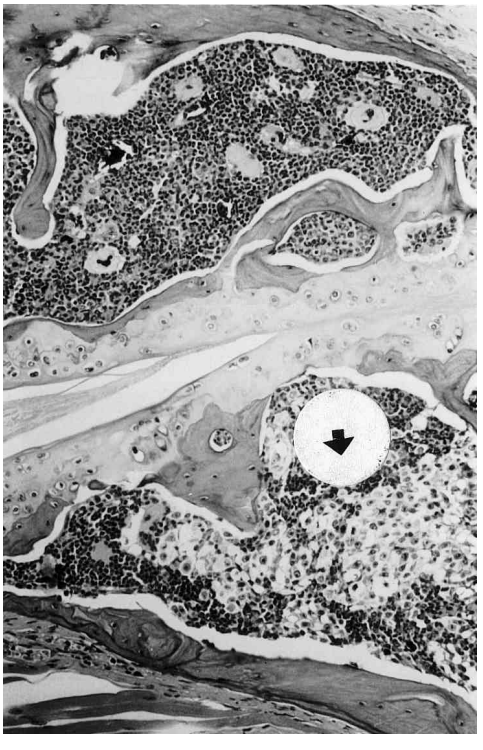

Fig. 7 This histologic section of the rib cage in a SCID mouse shows infiltrating human plasma cells (ARH-77) appearing as a pale patch of cells in the intermedullary cavity. (hematoxylin and eosin section, ×40)

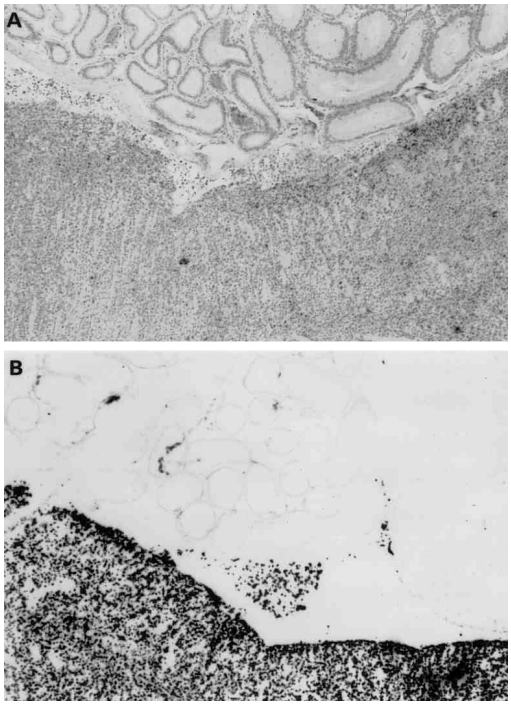

Fig. 8A Hematoxylin and eosin-stained section of SCID-human myeloma xenograft showing murine kidney (*top*) and ARH human myeloma tumor (*bottom*). **B** In situ hybridization of the same section to a DNA probe enriched for repetitive human DNA sequences. Murine kidney shows no staining while the tumor shows intense staining ($\times 40$).

take rate or dissemination pattern of the ARH-77/S or the ARH-D-60 cell lines. Figure 7 shows a section from the rib cage of a SCID mouse injected with ARH-D60 cells. Infiltrating human plasma cells appeared as a pale patch of cells in the intermedullary cavity. The human origin of the tumors was also confirmed through the use of in situ hybridization to a probe enriched for repetitive human *Alu* and *Kpn* DNA sequences as demonstrated in Fig. 8. When examined by immunohistochemistry, the SCID-human xenografts of ARH-D60 cells expressed P-glycoprotein in individual human myeloma cells as detected by the anti-P-glycoprotein antibody, JSB-1 (not shown).

Discussion

The resistance of tumor cells to the cytotoxic effects of chemotherapy continues to be a major obstacle to the successful treatment of human cancers. Chemotherapy is the primary treatment modality of multiple myeloma but, despite improvements in survival and quality of life, this remains an incurable disease in part due to the development of drug resistance. The evaluation of novel experimental therapeutic approaches for multiple myeloma has been hampered by the lack of an appropriate animal model. While murine models of myeloma are known, e.g. pristane-induced Balb/c peritoneal plasmacytomas and spontaneous C57BL marrow myelomas [2, 17, 34, 35], these systems do not specifically model human myeloma associated with drug resistance. We have recently developed a reproducible in vivo human xenograft model in SCID mice which utilizes both the RPMI 8226 human myeloma cell line and the P-glycoprotein-expressing MDR 8226/C1N subline, a derivative of the 8226/DOX40 MDR cell line [7].

This model has been initially used to evaluate chemosensitizers directed against P-glycoprotein [8, 9]. The combination of verapamil and doxorubicin resulted in both a decrease in light-chain excretion and an increase in survival of those animals bearing the 8226/C1N tumor, thus demonstrating its ability to offer an in vivo means of evaluating efficacy of new therapeutic approaches in MDR human myeloma. While we have observed a disseminated growth using the 8226/C1N cell line in our SCID xenograft model, unfortunately, this pattern has never included osteolytic lesions which are characteristic of human multiple myeloma [36]. Thus, the 8226-based model does not represent an orthotopic disease model. Recent studies have suggested the value of orthotopic models [25, 39]. As discussed by Fidler [25], the ideal in vivo model for the study of the basic biology and therapy of human tumors is one which allows the interaction of the tumor cell with the relevant microenvironment. While tumors implanted subcutaneously or intraperitoneally have been used for decades to study the biology of human tumors, these models fail to adequately reproduce an essential part of human tumor behavior and often drug responses do not match clinically observed patterns. The use of an orthotopic model more accurately reflects not only the tumor's biology but also the relevant pharmacokinetics of a particular compartment.

In this study we have developed two human myeloma cell lines derived from the parental ARH-77 cell line and selected for resistance to either doxorubicin or mitoxantrone. Both the ARH-D60 and ARM-80 cell lines display the MDR phenotype as evidenced by their cross-resistance profile and the expression of MDR1. Results from Southern blot analysis demonstrated amplification of the MDR1 gene in both cell lines, consistent with the karyotypic analysis which revealed an HSR located on the long arm of chromosome 7. There were several chromosomal alterations unique to the resistant sublines, but it is not clear whether these clonal changes were directly related to the resistant phenotype. Cytogenetic analysis of the ARH panel of cell lines demonstrated that gain of doxorubicin resistance correlated with gain of additional structural alterations (most notably the HSR bearing derivative chromosome 7) and that, further, reversion to a more sensitive phenotype (ARH-D60-Rev) correlated only with loss of the HSR chromosome.

Chromosome band 7q21 (the normal locus for MDR1 and MDR3) was part of a duplicated region and was a site of an HSR in the ARH-D60 and ARM-80 cell lines.

Drug accumulation was found to be decreased in both drug-resistant sublines as compared to the parental cell line and was increased by the addition of verapamil but not to parental levels. Verapamil was also ineffective in completely reversing drug resistance as determined by MTT cytotoxicity analysis. This is in contrast to the 8226/Dox human myeloma cell line in which resistance can be fully reversed by the addition of verapamil [6]. The relative, not absolute, reversal in the two ARH cell lines may correspond more closely to the observed clinical phenomenon of "escape" from chemosensitization seen in drug-resistant P-glycoprotein-positive human myeloma [18, 37]. Significant resistance to vinca alkaloids and taxol was observed for both the ARH-D60 and ARM-80 cells which, coupled with the inability of verapamil to completely reverse drug resistance, suggests the possibility that there may be multiple mechanisms of drug resistance operating in these cell lines.

When the ARH-D60 cells were maintained in drug-free medium for 28 weeks, the level of MDR1 expression decreased. This was consistent with the observed loss of resistance to doxorubicin. When the ARH-D60 cells were analyzed at 15 weeks out of drug, there was no evidence of a loss in expression of MDR1, nor alteration in the level of drug resistance. Interestingly, when the ARH-D60-Rev cells were pulsed with doxorubicin for 4 h prior to the isolation of RNA, there appeared to be a slight elevation in MDR1 message which was not accounted for by differences in RNA loading. Studies are currently underway to determine if the level of resistance in the ARM-80 cell line decreases when the cells are maintained for an extended period in drug-free medium.

In the current study, both the ARH-77/S and the ARH-D60 cell lines demonstrated growth in a disseminated manner in irradiated SCID mice, but not in unirradiated mice. Huang et al. [29] also observed that the parent ARH-77 cell line fails to grow in nonirradiated SCID mice. The difference in observed take rates between nonirradiated and irradiated animals likely lies in the ability of the radiation to reduce the numbers of NK cells in the SCID mice, thus resulting in a lower rejection rate and an increased take rate. Our studies demonstrated that when using irradiated SCID mice there was a 100% tumor take rate via the i.v. route and that the ARH-D60 cells grew in an orthotopic, marrow-involved pattern. In particular, these cell lines proliferated in the bone marrow of vertebrae and the bones of skull, resulting in osteolytic lesions following i.v. injection. Tumor cells of both the ARH-77/S and the ARH-D60 lines infiltrated the thoracolumbar vertebrae resulting in a compression of the spinal cord with concomitant hind leg paralysis. Cells also grew in various organs including the liver, kidney, peritoneum and skeletal muscle. All of the SCID xenograft tumors had the morphologic appearance of plasmacytomas. Immunophenotyping revealed that they were human in origin and were human kappa light-chain positive and lambda light-chain negative. Additionally, tumors derived from the ARH-D60 cell line were demonstrated to be P-glycoprotein positive. The marrow growth involvement is similar to that of human multiple myeloma in general and the pattern of wide-spread organ dissemination is consistent with the clinical pattern of the parental cell line being a plasma cell leukemia. The ARH-D60 cell line therefore grows in a more orthotopic manner in SCID mice than the 8226 cell line previously used in our SCID mouse xenograft model and represents an in vivo human–SCID P-glycoprotein-positive MDR multiple myeloma xenograft model which is closer to the marrow-based pathophysiology of human myeloma. In light of the possibility of multiple mechanisms of resistance, we are currently examining the suitability of the ARH-D60 cell line in our in vivo chemosensitivity model for reversal of MDR1 mediated drug resistance.

The SCID xenograft model was developed to assess the efficacy and toxicities of new chemotherapeutic agents and chemosensitizers directed against the P-glycoprotein-mediated MDR phenotype and should serve to complement current in vitro assays which are better suited to initially identify compounds effective in overcoming P-glycoprotein mediated drug resistance. The advantages of the SCID human myeloma xenograft model have been previously stated and allow for quantification of tumor burden via urinary monoclonal light-chain measurement and a reproducible, defined time frame of tumor growth and survival allowing for assessment of outcome in a speedy fashion. Measurements of serum immunoglobulin have been demonstrated to correlate with the total tumor burden in patients with IgG myeloma [37]. The measurement of human monoclonal light-chain in the urine is a noninvasive and sensitive means of assessing human tumor burden in a murine model. By quantitating changes in urinary light-chain values at the initiation of and during chemotherapy, the efficacy of a given treatment can be determined. One of the advantages of this model is that tumor growth and treatment effects can be assessed repeatedly by human monoclonal light-chain assays without relying solely on measurements such as the percentage increase in lifespan. Treatment can be initiated at a specific tumor burden, thus permitting a direct comparison of the effectiveness of chemotherapeutic agents used at the same extent of disease in each animal. This approach is preferable to the other models in which the tumor is treated at a predetermined time interval following the inoculation of a known number of tumor cells. In such systems the actual tumor burden in individual animals may vary considerably, thus complicating direct comparisons.

Our model permits the precise quantification of response and comparison of agents in mice with similar tumor burdens. Those compounds identified as promising on the basis of in vitro assays would then become candidates for in vivo evaluation of their ability to reverse P-glycoprotein-mediated drug resistance. The initial evaluation of chemosensitizers in our model has been performed using verapamil [8]. The combination of verapamil and doxorubicin resulted in both a decrease in light-chain excretion and an increase in survival of those animals bearing the 8226/C1N tumor.

In addition to evaluating drug efficacy, the SCID xenograft model allows investigators to examine pharmacokinetic and pharmacodynamic parameters, which are not easily studied in the in vitro setting, and to identify the limiting organ-specific toxicities resulting from the use of new chemomodulators. Indeed, we have used this model to identify increased toxicities in the SCID mouse as a consequence of the administration of doxorubicin and cyclosporin A [9].

Using this model, we may not be able to differentiate the effects of inhibition of P-glycoprotein from that of altered pharmacokinetics solely by examining changes in the urinary light-chain excretion nor by prolonged survival times. What we will be able to do, however, is to provide information relating to the efficacy or toxicities of a given compound under the actual conditions of its proposed use. Several studies have demonstrated that the use of chemomodulators directed against the P-glycoprotein may alter the pharmacokinetics of antineoplastic agents resulting in decreased clearance and/or increased area under the curve [16, 23, 31, 33]. Such reports are of importance due to the potential of increased toxicities when chemomodulators are utilized. In order to assess whether the observed effects of a compound being examined in our model are due to alterations in pharmacokinetics we will utilize measurements of tissue and plasma levels of the drugs as we have done previously [9].

In summary, these observations confirm that the SClD mouse is an excellent recipient for human multiple myeloma cells and that cell lines like ARH-D60 with specifically "engineered" features may present a truer pathophysiologic model of MDR myeloma than others currently available. This in vivo model should be useful not only for studying drug-resistant human multiple myeloma but also as a more general model of multiple myeloma providing a means to evaluate the effectiveness of various therapeutic strategies aimed at this disease and to elucidate the mechanisms by which myeloma cells may escape from chemosensitization.

Acknowledgements We thank Catherine Rangel and Yvette Furtiger for technical assistance with immunohistochemical staining; Yun Liu and Jin-Ming Yang for karyotype preparation; Abiodun Odeleye for assistance with animal studies, and Barbara Carolus of the Biotechnology Cell Sorting Facility of the University of Arizona for help with the flow cytometry studies.

References

1. Alexanian R, Barlogie B, Tucker S (1990) VAD-based regimens as primary treatment for multiple myeloma. Am J Hematol 33:86–89
2. Azar HA (1975) Experimental plasmacytomas in relation to human multiple myeloma. Ann Clin Lab Sci 4:157–163
3. Barlogie B, Smith L, Alexanian R (1984) Effective treatment of advanced multiple myeloma refractory to alkylating agents. N Engl J Med 310:1353–1356
4. Barlogie B, Epstein J, Selvanayagam P, Alexanian R (1989) Plasma cell myeloma – new biological insights and advances in therapy. Blood 73:865–879
5. Bellamy W, Dalton W (1994) Multidrug resistance in the laboratory and clinic. Adv Clin Chem 31:1-61
6. Bellamy WT, Dalton WS, Kailey JM, Gleason MC, McCloskey TM, Dorr RT, Alberts D (1988) Verapamil reversal of doxorubicin resistance in multidrug-resistant human myeloma cells and association with drug accumulation and DNA damage. Cancer Res 48:6365–6370
7. Bellamy WT, Odeleye A, Finley P, Huizenga E, Dalton W, Weinstein R, Hersh E, Grogan T (1993) An in vivo model of human multidrug-resistant multiple myeloma in SCID mice. Am J Pathol 142:691–698
8. Bellamy W, Odeleye A, Finley P, Huizenga B, Weinstein R, Grogan T (1993) An in vivo model of chemosensitization of multidrug resistant human myeloma cell line in SCID mice. Proc Am Assoc Cancer Res 34:319
9. Bellamy W, Peng Y, Odeleye A, Huizenga E, Xu M, Grogan T, Weinstein R (1994) The addition of cyclosporin A results in markedly elevated tissue levels of doxorubicin in the SCID mouse. Proc Am Assoc Cancer Res 35:354
10. Bergsagel DE (1989) Is aggressive chemotherapy more effective in the treatment of plasma cell myeloma? Eur J Cancer Clin Oncol 25:159–161
11. Burk KH, Drewinko B, Turjillo JM, Ahearn MJ (1978) Establishment of a human plasma cell line in vitro. Cancer Res 38:2508–2513
12. Camba L, Durie BG (1992) Multiple myeloma. New treatment options. Drugs 44:170–181
13. Carmichael J, DeGraff W, Gazdar A, Minna J, Mitchell J (1987) Evaluation of a tetrazolium-based semi-automatic colorimetric assay: assessment of chemosensitivity testing. Cancer Res 47:936–942
14. Chirgwin JM, Przybyla AE, MacDonald RJ, Rutter WJ (1979) Isolation of biologically active ribonucleic acid from sources enriched in ribonuclease. Biochemistry 18:5294–5299
15. Cole SP, Bhardwaj G, Gerlach JH, Mackie J, Grant CE, Almquist KC, Stewart AJ, Kruz EU, Duncan AM, Deeley RG (1992) Overexpression of a transporter gene in a multidrug-resistant human lung cancer cell line. Science 258:1650–1654
16. Colombo T, Zucchetti M, D'Incalci M (1993) Cyclosporin A induces drastic modifications in doxorubicin distribution in mice. Proc Am Assoc Cancer Res 34:322
17. Croese JW, Vas Nunes CM, Radl J, van den Enden-Vieveen MHM, Brondijk RJ, Boersma WJA (1987) The 5T2 mouse multiple myeloma model: characterization of 5T2 cells within the bone marrow. Br J Cancer 56:555–560
18. Dalton WS, Grogan TM, Meltzer PS, Scheper R, Durie B, Taylor C, Miller T, Salmon S (1989) Drug-resistance in multiple myeloma and non-Hodgkin's lymphoma: detection of P-glycoprotein and potential circumvention by addition of verapamil to chemotherapy. J Clin Oncol 7:415–424
19. Dalton WS, Grogan TM, Rybski JA, Scheper R, Richter L, Kailey J, Broxterman H, Pinedo H, Salmon S (1989) Immunohistochemical detection and quantitation of P-glycoprotein in multiple drug-resistant human myeloma cells: association with level of drug resistance and drug accumulation. Blood 73:747–752

20. Dalton WS, Grogan TM, Miller TP (1991) The role of P-glycoprotein in drug-resistant hematologic malignancies. Cancer Treat Res 57:187–208
21. Drewinko B, Mars W, Stragand JJ, Henderson DD, Latreille J, Barlogie B, Trujillo JM (1984) ARH-77, an established human IgG-producing myeloma cell line. II. Growth kinetics, clonogenic capacity, chalone production, xenogeneic transplantations, and response to melphalan. Cancer 54:1893–1903
22. Epstein J, Xiao HQ, Oba BK (1989) P-glycoprotein expression in plasma-cell myeloma is associated with resistance to VAD. Blood 74:913–917
23. Erlichman C, Moore M, Thiessen JJ, Kerr IG, Walker S, Goodman P, Bjarnason G, DeAngelis C, Bunting P (1993) Phase I pharmacokinetic study of cyclosporin A combined with doxorubicin. Cancer Res; 53:4837–4842
24. Feinberg AP, Vogelstein B (1983) A technique for radiolabeling DNA restriction endonuclease fragments to high specific activity. Anal Biochem 132:6–13
25. Fidler I (1990) Critical factors in the biology of human cancer metastasis. Cancer Res 50:6130–6138
26. Gerdes J, Lemke H, Baisch H, Wacker HH, Schwab U, Stein H (1984) Cell cycle analysis of a cell proliferation-associated human nuclear antigen defined by the monoclonal antibody Ki-67. J Immunol 133:1710–1715
27. Grogan T, Dalton W, Rybski J, Spier C, Meltzer P, Richter L, Pindur J, Cline A, Scheper R, Tsuruo T, Salmon S (1990) Optimization of immunocytochemical P-glycoprotein assessment in multidrug-resistant plasma cell myeloma using three antibodies. Lab Invest 63:815–824
28. Grogan TM, Spier CM, Salmon SE, Matzner M, Rybski J, Weinstein R, Scheper R (1993) P-glycoprotein expression in human plasma cell myeloma: correlation with prior chemotherapy. Blood 81:490–495
29. Huang Y-W, Richardson JA, Tong AW, Zhang B-Q, Stone MJ, Vitetta ES (1993) Disseminated growth of a human multiple myeloma cell line in mice with severe combined immunodeficiency disease. Cancer Res 53:1392–1396
30. ISCN (1985) An International System for Human Cytogenetic Nomenclature. Cytogenet Cell Genet 21:1–117
31. Kerr DJ, Graham J, Cummings J, Morrison JG, Thompson GG, Brodie MJ, Kaye SB (1986) The effect of verapamil on the pharmacokinetics of adriamycin. Cancer Chemother Pharmacol 18:239–242
32. Krishan A (1975) Rapid flow cytofluorometric analysis of mammalian cell cycle by propidium iodide staining J Cell Biol 66:188–193
33. Lum BL, Kaubisch S, Yahanda AM, Adler KM, Jew L, Ehsan MN, Brophy NA, Halsey J, Gosland MP, Sikic BI (1992) Alteration of etoposide pharmacokinetics and pharmacodynamics by cyclosporine in a phase I trial to modulate multidrug resistance. J Clin Oncol 10:1635–1642
34. Potter M, Boyce CR (1962) Induction of plasma-cell neoplasms in strain BALB/c mice with mineral oil and mineral oil adjuvants. Nature 193:1086–1087
35. Radl J, Croese JW, Zurcher C, Van den Enden-Vieveen MHM, de Leeuw AM (1988) Animal model of human disease multiple myeloma. Am J Pathol 132:593–597
36. Salmon SE, Cassady JR (1993) Plasma cell neoplasms. In: DeVita V, Hellman S. Rosenberg S (eds) Cancer: principles and practice of oncology, 4th edn. Lippincott, New York, pp 1984–2025
37. Salmon SE, Dalton WS, Grogan TM, Plezia P, Lenhert M, Roe DJ, Miller TP (1991) Multidrug resistant myeloma: laboratory and clinical effects of verapamil as a chemosensitizer. Blood 78:44–50
38. Thompson FH (1991) Cytogenetic methodological approaches and findings in human solid tumors. In: Barch M (ed) The A.C.T. Cytogenetics Laboratory Manual, 2nd edn. Raven Press, New York, pp 451–488
39. Togo S, Shimada H, Kubota T, Moossa AR, Hoffman RM (1995) Host organ specificity determines cancer progression. Cancer Res 55:681–684
40. Trent JM, Thompson FH (1987) Methods for chromosome Banding of human and experimental tumors in vitro. In: Gottesman MM (ed) Methods in Enzymology. Molecular genetics of mammalian cells. Vol. 151. Academic Press, San Diego, pp. 267–279
41. Ueda K, Clark DP, Chen CJ, Roninson IB, Gottesman MM, Pastan I (1987) The human multidrug resistance (mdr1) gene. cDNA cloning and transcription initiation. J Biol Chem 262:505–508